Inorganic Chemistry

Article

pubs.acs.org/IC

Influence of the Coordination Environment of Zinc(II) Complexes of Designed Mannich Ligands on Phosphatase Activity: A Combined Experimental and Theoretical Study

Ria Sanyal,[†] Averi Guha,[†] Totan Ghosh,[†] Tapan Kumar Mondal,[‡] Ennio Zangrando,*[,§] and Debasis Das*[,†]

[†]Department of Chemistry, University of Calcutta, 92, A. P. C. Road, Kolkata 700009, India

[‡]Department of Chemistry, Jadavpur University, Jadavpur, Kolkata 7000032, India

[§]Dipartimento di Scienze Chimiche e Farmaceutiche, University of Trieste, Via L. Giorgieri 1, 34127 Trieste, Italy

Supporting Information

ABSTRACT: A mononucleating (HL^1) and a dinucleating (HL^2) "end-off" compartmental ligand have been designed and synthesized by controlled Mannich reaction using *p*-cresol and bis(2-methoxyethyl)amine, and their formation has been rationalized. Six complexes have been prepared on treating HL^1 and HL^2 with $Zn^{II}X_2$ (X = Cl^-, Br^-, I^-) with the aim to investigate their hydrolytic activity on phosphoester bond cleavage. Interestingly, the mononucleating ligand was observed to yield dinuclear complexes, $[Zn_2(L^1)_2X_2]$ (**1**–**3**), while the potential dinucleating ligand generated mononuclear complexes, $[Zn(HL^2)X_2]$ (**4**–**6**). Four (**1**–**4**), out of six complexes studied, were characterized by single-crystal X-ray diffraction (XRD): the Zn ion exhibits trigonal bipyramidal and tetrahedral coordination spheres in the di- and mononuclear complex, respectively. The hydrolytic kinetics, followed spectrophotometrically with 4-nitrophenylphosphate (4-NPP) in buffered dimethylformamide (DMF) (97.5% DMF, v/v) because of solubility reasons, under excess substrate conditions (substrate:complex = 20:1), indicated that the complexes enormously accelerate the rate of phosphomonoester hydrolysis with first order rate constants (k_{cat}) in the range 2–10 s^{-1} at 25 °C. In each case kinetic data analyses have been run by Michaelis–Menten treatment. The efficacy in the order of conversion of substrate to product (*p*-nitrophenolate ion) follows the trend **1** > **2** > **3** > **4** > **5** > **6**, and the ratio of k_{cat} of an analogous dinuclear to mononuclear complex is ≃2. An electrospray ionization-mass spectrometry (ESI-MS) study has revealed the dissociation of the centrosymmetric dinuclear complex to two mononuclear species instead of a syn-cooperative catalysis. Density functional theory (DFT) calculations have been performed to rationalize our proposed mechanistic pathway for phosphatase activity. The comparative analysis concludes the following facts under experimental conditions: (1) the halide bound to the active site affects the overall rate in the order: Cl^- > Br^- > I^- regardless of nuclearity; (2) dinuclear complexes prevail over the mononuclear ones.

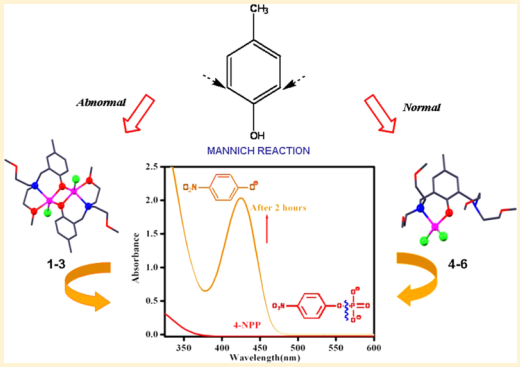

INTRODUCTION

Zinc, being one of the most biocompatible metals,[1−6] is present in all forms of life,[7−10] with an average adult human content of about 3 g of this metal.[11] This influence of zinc derives from its role in enzymes, with functions that are both structural and catalytic. Excellent Lewis acidity, capability of undergoing rapid ligand exchange, flat coordination hypersurface,[12−15] and free from any undesired redox activity make Zn^{II} the most obvious choice in hydrolytic enzymes.[16,17] It is now well documented that zinc enzymes play an important role in the cleavage of the P-OR bond in phosphates, $[(RO)PO_3]^{2-}$ and $[(RO)_2PO_2]^-$, as exemplified by their nuclease activity pertaining to the hydrolysis of DNA and RNA.[18,19] In nature, many enzymes that catalyze phosphate ester hydrolysis are activated by two or more metal ions. These include phosphate mono-, di-, and triesterases, all pertaining to the class of phosphatase enzymes,[20,21] which have evolved to catalyze the cleavage of both naturally occurring and synthetic phosphate esters.[22,23] These zinc enzymes can use external water molecules or internal alcoholic hydroxyl residues as nucleophiles to react with electrophilic substrates. In case of dinuclear sites, both metals are involved in the catalytic process: either one metal ion provides the nucleophile and the other coordinates the substrate or they may act cooperatively participating in substrate binding, activation, and cleavage.[24−26] This mutual action usually renders dinuclear complexes far more reactive than their mononuclear analogues.[27]

It is therefore evident that zinc plays multifaceted roles in biological systems, and a detailed understanding of these roles requires a correspondingly detailed appreciation of how the chemistry of zinc is modulated by its coordination environ-

Received: June 19, 2013
Published: December 19, 2013

   dx.doi.org/10.1021/ic4015493 | *Inorg. Chem.* 2014, 53, 85−96

ment. Many metal ion based model systems have been reported, and in most of the cases the ligands are tridentate or tetradentate Schiff-base ligands with free coordination sites of the metal cation.[28] Here our preliminary goal is to develop reactive chemical systems employing comparatively less explored ligands, Mannich base ligands that efficiently hydrolyze phosphate monoester bonds, and to study the roles of nuclearity, labile groups, geometry of the complexes, and so forth on the catalytic efficiency of the systems. In the present work, we have synthesized two phenolic ligands, namely, 2-[bis(2-methoxyethyl)aminomethyl]-4-methylphenol (HL^1) and 2,6-bis[bis(2-methoxyethyl)aminomethyl]-4-methylphenol (HL^2),[29−34] by properly tuning the progress of Mannich reaction to achieve the insertion of one or two pendant chelating arms. On complexation with ZnX_2 salts (X = Cl^-, Br^-, I^-) the former ligand generates dinuclear and the latter generates mononuclear complexes, a behavior that appears apparently anomalous. The solid-state structures of four complexes out of six have been authenticated by X-ray single cryatal structural analyses, and their solution phase structures have been established by UV−vis, electrospray ionization-mass spectrometry (ESI-MS), NMR spectra (DMF-d_7 and DMSO-d_6 as d-solvents), and by molar conductivity studies. Finally, phosphatase activity of those complexes has been thoroughly investigated using 4-nitrophenylphosphate as substrate in aqueous dimethylformamide (DMF) for all the complexes at 298 K. The role of halide ligands on the phosphatase activity has been explored, and probable mechanistic pathways involved in mono- and dinuclear Zn^{II} complexes have been proposed on the basis of density functional theory (DFT) calculations.

EXPERIMENTAL SECTION

Materials and Methods. (4-Nitrophenyl)phosphate was purchased from Aldrich. 4-NPP was recrystallized from ethanol/water before use. Reaction solutions for 4-NPP cleavage were prepared according to the standard sterile techniques. DMF was dried over CaH_2 for 2 days and then distilled under reduced pressure prior to use. The anhydrous zinc halide salts (analytical grade) were obtained from Merck. Common organic reagents and solvents used for synthesis were reagent grade which were obtained from commercial sources and redistilled before use. Water used in all physical measurement experiments was Milli-Q grade.

Elemental analyses (carbon, hydrogen, and nitrogen) were performed using a PerkinElmer 240C analyzer. Infrared spectra (4000−400 cm^{-1}) were recorded at 28 °C on a Shimadzu FTIR-8400S and PerkinElmer Spectrum Express Version 1.03 using both KBr-pellets and NaCl-plates as mediums. ^1H and ^{13}C NMR spectra (300 MHz) were recorded in $CDCl_3$ and $DCON(CD_3)_2$ solvents at 25 °C on a Bruker AV300 Supercon NMR spectrometer using the solvent signal as the internal standard in a 5 mm BBO probe. UV−visible spectra and kinetic traces were monitored with a Shimadzu 2450 UV/vis spectrophotometer equipped with multiple cell-holders and thermostat. Electrospray mass spectra were recorded on a Micromass Q-TOF mass spectrometer. Molar conductances were measured with a Systronics conductivity meter 306 at 25 °C.

Syntheses of Ligands. *Synthesis of HL^1.* To an ethanolic solution (50 mL) of *p*-cresol (30 mmol, 3.24 g), bis(2-methoxyethyl)amine (30 mmol, 3.99 gms) was added dropwise with constant stirring. After 30 min, 37% (w/v) formalin solution (30 mmol, 2.43 mL) was added to it. The resulting mixture was stirred for an additional 1 h at room temperature and then refluxed for 8 h. It was evaporated under reduced pressure, and the yellow oil was extracted with saturated brine solution and diethyl-ether several times. The organic phase was separated, dried with anhydrous $MgSO_4$, concentrated by evaporation of ether and subsequently vacuum-dried for the removal of last traces of water. Yield = 3.04 g (40%). Elemental analysis calcd (%) for $C_{14}H_{23}N_1O_3$: C 66.37, H 9.15, N 5.53, O 18.95; found C 65.99, H 9.75, N 5.80, O 19.18 ^1H NMR (300 MHz, $CDCl_3$, 25 °C): δ = 2.2(s, 3H; ph-$\underline{CH_3}$), 2.83(t, 4H; N-$\underline{CH_2}$-CH_2), 3.33(s, 6H; O-$\underline{CH_3}$), 3.54(t, 4H; N−CH_2-$\underline{CH_2}$), 3.81(s, 2H; ph-$\underline{CH_2}$-N), 7.2(d, 1H; Ar), 7.26(s, 1H; *o* to CH_2−N), 7.43 ppm(d, 1H; *o* to phenolic−OH); ^{13}C NMR (300 MHz, DMSO-d_6, 25 °C): δ = 20.13(1C, ph-Me), 52.61(2C, O-Me), 56.47(1C, ph-$\underline{CH_2}$−N), 58.05(2C, N-$\underline{CH_2}$−CH_2), 69.6(2C, N−CH_2-$\underline{CH_2}$), 115.08(1C, Ar), 127.07(1C, Ar), 128.57(1C, Ar), 129.49(1C, Ar), 129.74(1C, Ar), 154.97(1C, $\underline{Ar}$−OH); IR data (NaCl plate): γ bar = 768, 818, 1117, 1256, 1600, 2923 cm^{-1}; UV/vis (DMF): $\lambda_{max}(\varepsilon)$ = 253.1(2800), 284.3(5400), 339.4 nm (2 L mol^{-1} cm^{-1}).

Synthesis of HL^2. To an ethanolic solution (30 mL) of *p*-cresol (30 mmol, 3.24 gms), bis(2-methoxyethyl)amine (90 mmol, 11.99 gms) was added dropwise with constant stirring. After 30 min, 37% (w/v) formalin solution (90 mmol, 7.5 mL) was added to it. The resulting mixture was stirred for an additional 1 h at room temperature and then refluxed for 24 h. It was followed by the same workup as HL^1. The liquid ligand was further purified by flash column chromatography (silica gel, hexane: ethylacetate: triethylamine =100: 5: 1) to afford the desired β-aminophenol.

Yield = 3 g (25%). Elemental analysis calcd (%) for $C_{21}H_{38}N_2O_5$: C 63.29, H 9.61, N 7.03, O 20.07; found: C 63.42, H 9.49, N 7.16, O 19.93.

^1H NMR (300 MHz, $CDCl_3$, 25 °C): δ = 2.22(s, 3H; ph-$\underline{CH_3}$), 2.83(t, 8H; N-$\underline{CH_2}$-CH_2), 3.34(s, 12H; O-$\underline{CH_3}$), 3.55(t, 8H; N−CH_2-$\underline{CH_2}$), 3.8(s, 4H; ph-$\underline{CH_2}$-N), 6.96 ppm(s, 2H; Ar); ^{13}C NMR (300 MHz, DMSO-d_6, 25 °C): δ = 20.27(1C, ph-Me), 52.41(4C, O-Me), 56.45(2C, ph-$\underline{CH_2}$−N), 58.10(4C, N-$\underline{CH_2}$−CH_2), 69.50(4C, N−CH_2-$\underline{CH_2}$), 115.04(1C, Ar), 127.17(2C, Ar), 129.39(2C, Ar), 155.28(1C, $\underline{Ar}$−OH); IR data (NaCl plate): γ bar= 773, 821, 1115, 1255, 1367, 1463, 1609, 2876 cm^{-1}; UV/vis (DMF): $\lambda_{max}(\varepsilon)$ = 254.3(2400), 287.1(5600), 435.7 nm (2 L mol^{-1} cm^{-1}).

Synthesis of Zinc(II) Complexes. *Synthesis of $[Zn_2L_1^2Cl_2]$ (1).* To a methanolic solution (25 mL) of HL^1 (0.5 mmol, 126.5 mg), a methanolic solution (10 mL) of anhydrous zinc chloride (0.5 mmol, 112.6 mg) was added. The light yellow reaction mixture was refluxed for 2 h, cooled to room temperature, filtered and kept in a beaker. After 1 day, two kinds of crystals were observed in the colorless solution. They were carefully separated under a microscope with the following result: (1) colorless needle-shaped and (2) colorless square-shaped single crystals.

Yield = 72 mg (41%). Elemental analysis calcd (%) for $C_{28}H_{44}Cl_2N_2O_6Zn_2$: C 47.62, H 6.28, Cl 10.04, N 3.97, O 13.59, Zn 18.52; found: C 47.69, H 6.13, Cl 10.31, N 3.90, O 13.29, Zn 18.68; ^1H NMR (300 MHz, DMF-d_7, 25 °C): δ = 2.25(s, 6H; ph-$\underline{CH_3}$), 2.84(t, 8H; N-$\underline{CH_2}$-CH_2), 3.02(s, 12H; O-$\underline{CH_3}$), 3.38(t, 8H; N−CH_2-$\underline{CH_2}$), 3.92(s, 4H; ph-$\underline{CH_2}$-N), 6.8(d, 2H; Ar), 7.22(d, 2H; *o* to CH_2−N), 7.29 ppm(s, 2H; *o* to phenolic−OH); ^{13}C NMR (300 MHz, DMSO-d_6, 25 °C): δ = 20.18(1C, ph-Me), 52.60(2C, O-Me), 56.40(1C, ph-$\underline{CH_2}$−N), 58.07(2C, N-$\underline{CH_2}$−CH_2), 69.57(2C, N−CH_2-$\underline{CH_2}$), 115.33(1C, Ar), 122.88(1C, Ar), 127.10(1C, Ar), 128.59(1C, Ar), 129.53(1C, Ar), 154.91(1C, $\underline{Ar}$−OH); ESI-MS *m/z*: Calcd for $[C_{14}H_{23}Cl_1N_1O_3Zn_1]^+$ = 354.148, Found = 353.98; FT-IR data (KBr pellet): γ bar = 836, 1021, 1105, 1270, 1491, 2370, 2924 cm^{-1}. UV/vis (DMF): $\lambda_{max}(\varepsilon)$ = 237.9(5000), 266.4(6600), 285.5 nm (6000 L mol^{-1} cm^{-1}).

Synthesis of $[Zn_2L_1^2Br_2]$ (2). This was prepared by the same procedure as above by using anhydrous zinc bromide as the metal salt. After 3 days, colorless and rhombic single crystals appeared in an yellow oil. It was washed with cold methanol and ether to obtain good crystals of X-ray crystallographic quality. Yield = 89 mg (45%). Elemental analysis calcd (%) for $C_{28}H_{44}Br_2N_2O_6Zn_2$: C 42.29, H 5.58, Br 20.10, N 3.52, O 12.07, Zn 16.45; found: C 42.18, H 5.65, Br 20.35, N 3.49, O 11.81, Zn 16.52; ^1H NMR (300 MHz, DMF-d_7, 25 °C): δ = 2.24(s, 6H; ph-$\underline{CH_3}$), 2.86(t, 8H; N-$\underline{CH_2}$-CH_2), 3.04(s, 12H; O-$\underline{CH_3}$), 3.38(t, 8H; N−CH_2-$\underline{CH_2}$), 3.95(s, 4H; ph-$\underline{CH_2}$-N), 6.77(d, 2H; Ar), 7.2(d, 2H; *o* to CH_2−N), 7.28 ppm(s, 2H; *o* to phenolic−OH); ^{13}C NMR (300 MHz, DMSO-d_6, 25 °C): δ = 20.10(1C, ph-Me), 52.65(2C, O-Me), 56.57(1C, ph-$\underline{CH_2}$−N), 58.13(2C, N-$\underline{CH_2}$−CH_2),

dx.doi.org/10.1021/ic4015493 | *Inorg. Chem.* 2014, 53, 85−96

Table 1. Crystallographic Data and Details of Refinement for Complexes 1−4

	1	2	3	4
empirical formula	$C_{28}H_{44}Cl_2N_2O_6Zn_2$	$C_{28}H_{44}Br_2N_2O_6Zn_2$	$C_{28}H_{44}I_2N_2O_6Zn_2$	$C_{21}H_{38}Cl_2N_2O_5Zn$
Fw	706.29	795.21	889.19	534.80
crystal system	monoclinic	monoclinic	monoclinic	triclinic
space group	$P2_1/n$	$P2_1/c$	$P2_1/c$	$P\bar{1}$
a, Å	9.9384(3)	9.936(3)	9.929(5)	9.161(4)
b, Å	15.8724(5)	15.907(4)	15.766(8)	9.568(4)
c, Å	11.2234(3)	11.429(3)	11.506(6)	16.493(7)
α, deg				84.493(5)
β, deg	115.3530(10)	115.753(3)	114.326(5)	88.106(5)
γ, deg				63.801(4)
V, Å^3	1599.93(8)	1626.9(8)	1641.3(14)	1291.0(9)
Z	2	2	2	2
D_{calcd}, g cm^{-3}	1.466	1.623	1.799	1.376
M(Mo−Kα), mm^{-1}	1.708	3.971	3.383	1.190
F(000)	736	808	880	564
θ range, deg	2.30−30.51	2.28−24.97	2.33−26.23	1.24−24.72
no. of reflns collcd	21033	10834	9950	8143
no. of indep reflns	4878	2839	3048	4239
Rint	0.0244	0.0635	0.1269	0.0445
no. of reflns ($I > 2\sigma(I)$)	4051	2337	2183	3304
refined params	181	181	184	288
goodness-of-fit (F^2)	1.030	1.048	1.024	1.043
R1, wR2 ($I > 2\sigma(I)$)[a]	0.0334, 0.0884	0.0450, 0.1160	0.0615, 0.1336	0.0605, 0.1564
residuals, e/Å^3	0.711, −0.522	0.901, −0.728	1.393, −0.997	0.638, −0.402

[a] $R1 = \sum||F_o| - |F_c||/\sum|F_o|$, $wR2 = \{\sum[w(F_o^2 - F_c^2)^2]/\sum[w(F_o^2)^2]\}^{1/2}$.

69.41(2C, N−CH_2-$\underline{C}H_2$), 115.19(1C, Ar), 127.07(1C, Ar), 128.48(1C, Ar), 129.56(1C, Ar), 129.69(1C, Ar), 154.88(1C, $\underline{Ar}$−OH); ESI-MS m/z: Calcd for $[C_{14}H_{23}Br_1N_1O_3Zn_1]^+$ = 398.613, Found = 398.02; FT-IR data (KBr pellet): γ bar = 796, 1022, 1109, 1271, 1491, 1610, 2927 cm^{-1}. UV/vis (DMF): $\lambda_{max}(\varepsilon)$ = 239.5(4200), 266.7(6800), 285.8 nm (5800 L mol^{-1} cm^{-1}).

*Synthesis of $[Zn_2L_1^2I_2]$ (**3**).* Anhydrous zinc iodide (1 mmol, 319.19 mg) in acetonitrile (5 mL) was added dropwise to an acetonitrile solution (10 mL) of the ligand L^1 (1 mmol, 253 mg), and the mixture was stirred very slowly for 30 min. The resulting yellow solution was filtered. After 6 h, off-white colored microcrystalline square-shaped crystals were formed in it. Yield = 112 mg (50%). Elemental analysis calcd (%) for $C_{28}H_{44}I_2N_2O_6Zn_2$: C 37.82, H 4.99, I 28.54, N 3.15, O 10.80, Zn 14.71; found: C 37.63, H 5.16, I 29.42, N 2.76, O 10.52, Zn 14.51; ^{1}H NMR (300 MHz, DMF-d_7, 25 °C): δ = 2.24(s, 6H; ph-$\underline{CH_3}$), 2.85(t, 8H; N-$\underline{CH_2}$-CH_2), 3.03(s, 12H; O-$\underline{CH_3}$), 3.37(t, 8H; N−CH_2-$\underline{CH_2}$), 3.91(s, 4H; ph-$\underline{CH_2}$-N), 6.83(d, 2H; Ar), 7.24(d, 2H; o to CH_2−N), 7.25 ppm(s, 2H; o to phenolic−OH); ^{13}C NMR (300 MHz, DMSO-d_6, 25 °C): δ = 20.14(1C, ph-Me), 52.68(2C, O-Me), 56.30(1C, ph-$\underline{C}H_2$−N), 58.09(2C, N-$\underline{C}H_2$−CH_2), 69.71(2C, N−CH_2-$\underline{C}H_2$), 114.98(1C, Ar), 126.91(1C, Ar), 128.64(1C, Ar), 129.33(1C, Ar), 129.78(1C, Ar), 154.91(1C, $\underline{Ar}$−OH); ESI-MS m/z: Calcd for $[C_{14}H_{23}I_1N_1O_3Zn_1]^+$ = 445.603, Found = 445.09; FT-IR data (KBr pellet): γ bar = 743, 1022, 1115, 1271, 1492, 1610, 2877 cm^{-1}; UV/vis (DMF): $\lambda_{max}(\varepsilon)$ = 238.6(5200), 266.4(7400), 285.8 nm (6400 L mol^{-1} cm^{-1}).

*Synthesis of $[Zn(HL^2)Cl_2]$ (**4**).* To a solution of ligand L^2 (1 mmol, 398 mg) in methanol (25 mL), methanolic anhydrous $ZnCl_2$ (2.5 mmol, 340.5 mg) was added (10 mL) and refluxed for 1 h. It was filtered, and ∼500 mg of white powder was collected. It was air-dried and redissolved in the mixed solvent dimethylformamide/water (9:1). Colorless rhombic crystals were formed after 1 month which were washed with ether to obtain single crystals of good crystallographic quality. Yield = 213 mg (40%). Elemental analysis calcd (%) for $C_{21}H_{38}Cl_2N_2O_5Zn$: C 47.16, H 7.16, Cl 13.26, N 5.24, O 14.96, Zn 12.23; found: C 47.10, H 7.25, Cl 13.21, N 5.15, O 15.0, Zn 12.29. ^{1}H NMR(300 MHz, DMF-d_7, 25 °C): δ = 2.25(s, 3H; ph-$\underline{CH_3}$), 2.84(t, 8H; N-$\underline{CH_2}$-CH_2), 3.02(s, 12H; O-$\underline{CH_3}$), 3.38(t, 8H; N−CH_2-$\underline{CH_2}$), 3.92(s, 4H; ph-$\underline{CH_2}$-N), 6.94 ppm(s, 2H; Ar); ^{13}C NMR (300 MHz, DMSO-d_6, 25 °C): δ = 20.20(1C, ph-Me), 52.41(4C, O-Me), 56.42(2C, ph-$\underline{C}H_2$−N), 58.23(4C, N-$\underline{C}H_2$−CH_2), 69.58(4C, N−CH_2-$\underline{C}H_2$), 115.34(1C, Ar), 127.07(2C, Ar), 129.37(2C, Ar), 155.61(1C, $\underline{Ar}$−OH); ESI-MS m/z: Calcd for $[C_{21}H_{38}Cl_1N_2O_5Zn]^+$=499.347, Found = 499.257; FT-IR data (KBr pellet): γ bar = 563, 1117, 1197, 1266, 1370, 1475, 2925 cm^{-1}; UV/vis (DMF): $\lambda_{max}(\varepsilon)$ = 234.4(3200), 284.9(5000), 317.4 nm (1100 L mol^{-1} cm^{-1}).

*Synthesis of $[Zn(HL^2)Br_2]$ (**5**).* It was synthesized by the same procedure as complex **4**. The crystalline compound was recrystallized from DMF-H_2O twice and used for further analysis as no single crystal was obtained in this case. Yield = 217 mg (35%). Elemental analysis calcd (%) for $C_{21}H_{38}Br_2N_2O_5Zn$: C 40.44, H 6.14, Br 25.62, N 4.49, O 12.83, Zn 10.48; found: C 40.34, H 6.25, Br 25.75, N 4.41, O 12.74, Zn 10.51. ^{1}H NMR(300 MHz, DMF-d_7, 25 °C): δ = 2.24(s, 3H; ph-$\underline{CH_3}$), 2.86(t, 4H; N-$\underline{CH_2}$-CH_2), 3.04(s, 6H; O-$\underline{CH_3}$), 3.38(t, 4H; N−CH_2-$\underline{CH_2}$), 3.95(s, 2H; ph-$\underline{CH_2}$-N), 6.96 ppm(s, 2H; Ar); ^{13}C NMR (300 MHz, DMSO-d_6, 25 °C): δ = 20.32(1C, ph-Me), 52.45(4C, O-Me), 56.29(2C, ph-$\underline{C}H_2$−N), 58.21(4C, N-$\underline{C}H_2$−CH_2), 69.47(4C, N−CH_2-$\underline{C}H_2$), 115.30(1C, Ar), 126.91(2C, Ar), 129.39(2C, Ar), 155.70(1C, $\underline{Ar}$−OH); ESI-MS m/z: Calcd for $[C_{21}H_{38}Br_1N_2O_5Zn]^+$ = 543.796, Found = 542.17; FT-IR data (KBr pellet): γ bar = 551, 1100, 1183, 1253, 1362, 1461, 2910 cm^{-1}; UV/vis (DMF): $\lambda_{max}(\varepsilon)$ = 234.7(3000), 284.9(4800), 340.1 nm (600 L mol^{-1} cm^{-1}).

*Synthesis of $[Zn(HL^2)I_2]$ (**6**).* It was also synthesized by the same procedure as complex **4**. A good quality crystalline compound was obtained and well characterized. Yield = 387 mg (54%). Elemental analysis calcd (%) for $C_{21}H_{38}I_2N_2O_5Zn$: C 35.14, H 5.34, I 35.36, N 3.90, O 11.15, Zn 9.11; found: C 35.09, H 5.28, I 35.41, N 3.93, O 11.09, Zn 9.20. ^{1}H NMR(300 MHz, DMF-d_7, 25 °C): δ = 2.24(s, 3H; ph-$\underline{CH_3}$), 2.85(t, 4H; N-$\underline{CH_2}$-CH_2), 3.03(s, 6H; O-$\underline{CH_3}$), 3.37(t, 4H; N−CH_2-$\underline{CH_2}$), 3.91(s, 2H; ph-$\underline{CH_2}$-N), 6.98 ppm(d, 1H; Ar); ^{13}C NMR (300 MHz, DMSO-d_6, 25 °C): δ = 20.15(1C, ph-Me), 52.55(4C, O-Me), 56.48(2C, ph-$\underline{C}H_2$−N), 58.17(4C, N-$\underline{C}H_2$−CH_2), 69.50(4C, N−CH_2-$\underline{C}H_2$), 115.39(1C, Ar), 127.08(2C, Ar), 129.29(2C, Ar), 155.60(1C, $\underline{Ar}$−OH); ESI-MS m/z: Calcd for $[C_{21}H_{38}I_1N_2O_5Zn]^+$ = 590.798, Found = 592.08; FT-IR data (KBr

dx.doi.org/10.1021/ic4015493 | Inorg. Chem. 2014, 53, 85−96

pellet): γ bar = 798, 1021, 1115, 1271, 1491, 1349, 2900 cm^{-1}; UV/vis (DMF): $\lambda_{max}(\varepsilon)$ = 234.4(3400), 284.9(5400), 316.5 nm (1200 L mol^{-1} cm^{-1}).

X-ray Data Collection. Crystal structure analyses of all compounds reported (**1**–**4**) were carried out at room temperature on a Bruker Smart Apex diffractometer equipped with CCD and Mo–Kα radiation (λ = 0.71073 Å). Cell refinement, indexing, and scaling of the data sets were done by using the Bruker Smart Apex and Bruker Saint packages.[35] All the structures were solved by direct methods and subsequent Fourier analyses[35] and refined by the full-matrix least-squares method based on F^2 with all observed reflections.[36] The ΔF map revealed the methoxy group -O(3)–C(13)H_2- of **1** and **2** disordered over two positions of occupancy x and $1 - x$. The x parameter was refined to 0.540(6) and 0.534(15), respectively, keeping these atoms isotropically. The H atom of the protonated amine in **4** was located on the Fourier map, all the other were fixed at geometrical positions. All the calculations were performed using the WinGX System, Ver 1.80.05.[37] Crystal data and details of refinements are given in Table 1.

Kinetic Measurements of the Hydrolysis of 4-NPP in 97.5% (v/v) DMF-H_2O. Disodium (4-nitrophenyl)phosphate (4-NPP) hexahydrate was used as the substrate. The solutions of substrate 4-NPP and Zn complexes in the mixed solvent were freshly prepared, and the total volume of the reaction mixture was maintained as 2 mL. An initial screening of the hydrolytic tendencies of all the metal-complexes was performed till 2% formation of *p*-nitrophenolate (~2 h) and then their kinetic data was collected. The hydrolysis rate of 4-NPP in the presence of complexes **1**–**6** was measured by an initial rate method following the increase in the 427 nm absorption due to the released 4-nitrophenolate ion in aqueous DMF (ε, 18500 M^{-1} cm^{-1}) at 25 °C . For wavelength scan, spectra were recorded from a solution having 1 mmol 4-NPP and 0.05 mmol Zn complex for 2 h. Kinetic experiments were done both at conditions of excess substrate and excess Zn complex keeping the other constant. Herein we report only the former data. The study comprised 5 sets having the catalyst concentration as 0.05 mmol and substrate as 0.5 (10 equiv), 0.7 (14 equiv), 1.0 (20 equiv), 1.2 (24 equiv) and 1.5 (30 equiv) mmol. The reactions were initiated by injecting 0.04 mL of complex (2.5×10^{-3} M) into 1.96 mL of 4-NPP solution, and the spectrum was recorded only after fully mixing at 25 °C. The visible absorption increase was recorded for a total period of 30 min at an interval of 5 min. All measurements were performed in triplicate, and the average values were adopted. The reactions were corrected for the degree of ionization of the 4-nitrophenol at 25 °C using the molar extinction coefficients for 4-nitrophenolate at 427 nm.[38] The final A_∞ values for each set were obtained after 2 days at 25 °C.

Computational Method. Geometry optimizations of complex **1** and **4** along with the possible intermediates in the proposed mechanisms were carried out using the DFT computational technique at the B3LYP level[39] in the Gaussian03 (G03)[40] software. For C, H, N, O, P, and Cl the 6-31G(d) basis sets were used, while for Zn the LANL2DZ basis set with effective core potential was employed.[41] The vibrational frequency calculations were performed to ensure that the optimized geometries represent the local minima and there are only positive eigenvalues.

RESULTS AND DISCUSSION

Design, Rationalization, and Characterization of Ligands. Mannich reaction is a relevant organic reaction for C–C bond formation widely used in the synthesis of nitrogenous molecules especially secondary and tertiary amine derivatives and applied as a key step in the synthesis of many bioactive molecules and complex natural products.[42,43] Foremost we had aspired to the synthesis of a conventional phenolic ligand by this age-old reaction with maximum yield and purity. The protocol requires a secondary amine [bis(2-methoxyethyl)-amine in our case] and formaldehyde on one side and an activated phenyl ring [*p*-cresol in our case] on the other for the occurrence of aromatic electrophilic substitution reaction. On monitoring the status of the reaction repeatedly for 30 h at an interval of 2 h, we found that the reaction proceeds through an intermediate that can be isolated and is a likely potent pentadentate ligand. Henceforth we proceeded in obtaining the two products independently in pure form.

Thus, starting from *p*-cresol with bis(2-methoxyethyl)amine and appropriate reaction conditions described below, two different types of end-off compartmental ligands have been synthesized, HL^1 and HL^2, having a NO_3 and N_2O_5 donor set, respectively (Figure 1).

These Mannich base ligands are actually produced in the reaction mixture by mono- and dicondensation of the electrophilic species generated in situ in presence of a protic solvent like ethanol. When the methylene iminium ion and *p*-

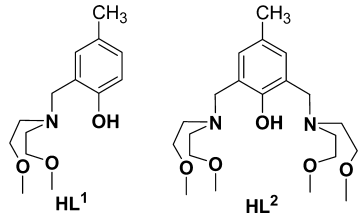

Figure 1. Designed ligands with NO_3 and N_2O_5 donor sets obtained by proper tuning of the Mannich reaction.

Scheme 1. Proposed Mechanistic Pathway for the Synthesis of Ligands HL^1 and HL^2 in Dry Ethanol by Controlled Mannich Reaction

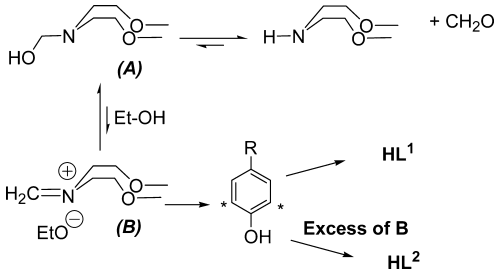

Scheme 2. Metal Incorporation Reaction Leading to the 2:2 Dinuclear $[Zn_2(L^1)_2X_2]$ (1–3) and 1:1 Mononuclear Metal-Complexes $[Zn(HL^2)X_2]$ (4–6)

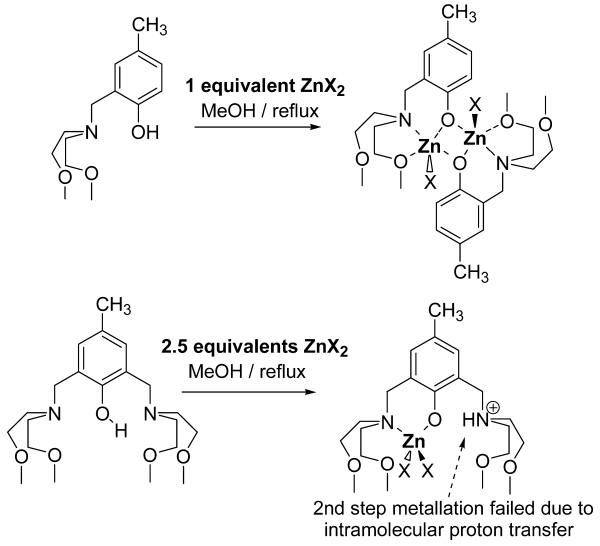

dx.doi.org/10.1021/ic4015493 | Inorg. Chem. 2014, 53, 85–96

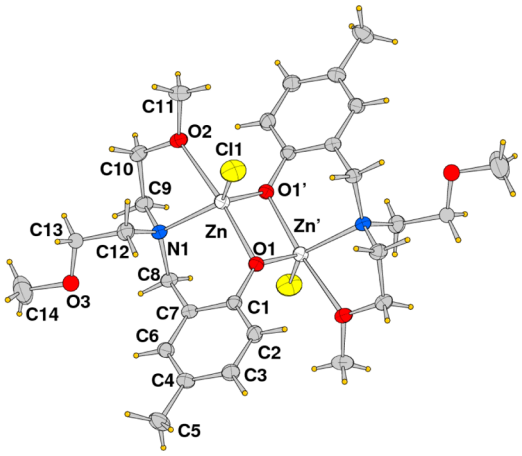

Figure 2. ORTEP view (35% ellipsoid probability) of compound **1** with atom labels of the crystallographic independent part. Of the disordered O3/C13 fragments, atoms at higher occupancy are shown (53%). The same numbering scheme of the ligand is applied to complexes **2** and **3**.

Table 2. Selected Bond Distances (Å) and Angles (deg) for Compounds 1−3[a]

	1 (X = Cl)	**2** (X = Br)	**3** (X = I)
Zn−N(1)	2.1157(14)	2.114(4)	2.093(6)
Zn−O(1)	2.0643(11)	2.059(3)	2.032(5)
Zn−O(1)#1	1.9727(12)	1.967(3)	1.941(5)
Zn−O(2)	2.3025(13)	2.296(3)	2.283(5)
Zn−X(1)	2.2068(6)	2.3412(9)	2.5085(13)
Zn−Zn#1	3.1081(4)	3.1032(11)	3.071(2)
N(1)−Zn−O(1)	93.08(5)	93.15(13)	93.3(2)
N(1)−Zn−O(1)#1	113.80(5)	114.69(14)	116.1(2)
N(1)−Zn−O(2)	75.84(5)	76.10(12)	76.3(2)
N(1)−Zn−X(1)	124.13(4)	124.09(10)	123.63(16)
O(1)−Zn−O(1)#1	79.34(5)	79.19(13)	78.8(2)
O(1)−Zn−O(2)	160.20(6)	160.05(13)	159.2(2)
O(1)−Zn−X(1)	106.17(4)	105.05(10)	104.12(16)
O(1)#1−Zn−O(2)	90.06(5)	89.96(12)	89.5(2)
O(1)#1−Zn−X(1)	121.02(4)	120.45(10)	119.69(16)
X(1)−Zn−O(2)	93.61(4)	94.88(9)	96.64(16)

[a]Primed atoms at $-x,-y,-z+2$ for **1**; at $-x+1,-y,-z$ for **2**; at $-x+1,-y,-z+1$ for **3**.

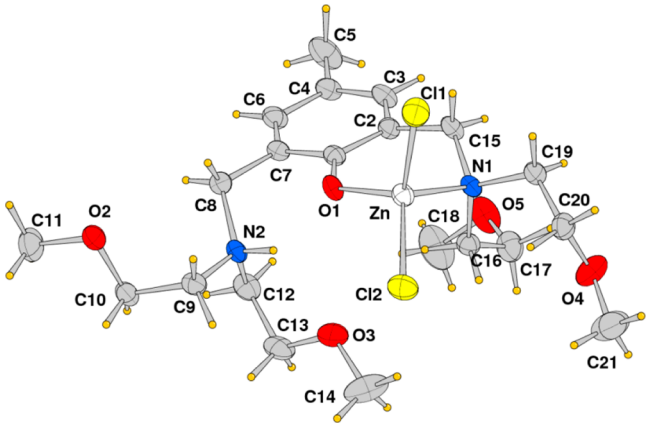

Figure 3. ORTEP view (35% ellipsoid probability) of compound **4**.

Table 3. Selected Bond Distances (Å) and Angles (deg) for Mononuclear Compound 4

	4 (X = Cl)
Zn−N(1)	2.092(4)
Zn−O(1)	1.926(3)
Zn−X(1)	2.2304(17)
Zn−X(2)	2.2289(17)
N(1)−Zn−O(1)	93.86(15)
N(1)−Zn−X(1)	106.40(12)
N(1)−Zn−X(2)	115.14(13)
O(1)−Zn−X(1)	114.57(13)
O(1)−Zn−X(2)	112.01(12)

Table 4. Hydrogen Bond Geometry (Å/deg) in Complex 4

complex	D−H	*d*(D−H)	*d*(H··A)	∠DHA	*d*(D··A)	A
4	N2−H	0.85(6)	1.96(6)	139(6)	2.659(6)	O1

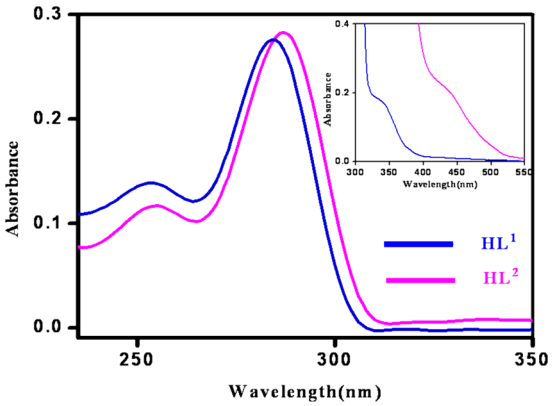

Figure 4. UV−vis spectra of the ligands in DMF at 5×10^{-5}(M). Inset shows the UV spectra at 0.1(M) concentration.

cresol are present in equimolar amount (*p*-cresol: amine: formalin =1: 1: 1) and the reflux time is limited to a few hours, the product is exclusively the single-side Mannich product. This can be explained assuming that the product attains a high degree of stability through intramolecular hydrogen bonding leading to a 6-membered chelate. Thus, the product in this case is less reactive than the reactant and hence reaction proceeds on the latter. On the other hand with a large excess of the electrophile generating species in the reaction mixture (*p*-cresol:amine:formalin =1:3:3) and a prolonged reaction time (ca. 1 day), the reaction proceeds further on the former single-arm Mannich molecule leading to a double-side condensation, which is actually the conventional product. Since some amount of the intermediate still remains in equilibrium despite enforcing the reaction, column chromatographic separation is required to obtain the pure ligand.

Synthesis, Rationalization, and Characterization of Zn^{II} Metal-Complexes. The treatment of the two ligand systems with anhydrous Zn-dihalide salts (i.e., $ZnCl_2$, $ZnBr_2$, and ZnI_2) led to the isolation of six complexes: four of which were structurally characterized by single crystal X-ray diffraction, and two were confirmed by elemental analysis and conventional spectroscopic techniques. The structure analyses (vide infra) reveal that the ligand HL^1, which is apparently mononucleating, gave rise to dinuclear Zn-complexes of close comparable structure, irrespective of the anion used. On the contrary, HL^2 which is distinctly a dinucleating ligand,

dx.doi.org/10.1021/ic4015493 | *Inorg. Chem.* 2014, 53, 85−96

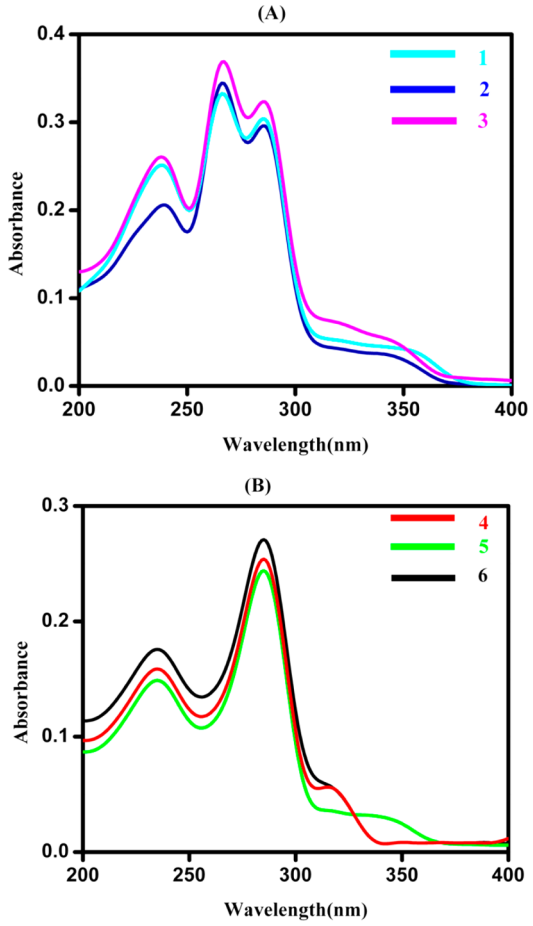

Figure 5. UV−vis spectra of the metal-complexes **1**−**3** (A) and **4**−**6** (B) in DMF at 5×10^{-5}(M) concentration.

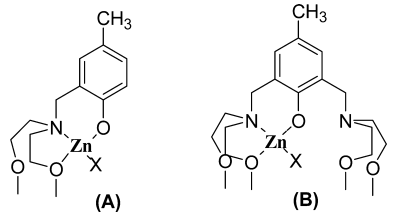

Figure 6. Probable solution state structures of complex **1**−**3** (A) and **4**−**6** (B) in DMF where X = Cl^- (**1**, **4**), Br^- (**2**, **5**), and I^- (**3**, **6**).

produced mononuclear Zn-complexes. We presume that the complex nuclearity is addressed by the strength of haloic and nitric acids (compared to acetates) and hence a high concentration of protons in the vicinity of the second nitrogen donor. Thus this atom becomes deactivated by intra- or intermolecular proton transfer (the former being kinetically and thermodynamically more favorable) because of hard−hard interaction hampering its coordination to another metal ion. Moreover in the case of the reaction of HL[1] with $ZnCl_2$ two crystal forms were obtained. Since these are close comparable dinuclear complexes, we have reported only the structure of that having one independent centrosymmetric complex. Since the strength of haloic acids follow the trend HI > HBr > HCl, we can be sure about the mononuclearity of complex **5** and **6** (no crystal structure given) in addition to the other analyses done, ruling out any similarity with the complex reported by Yamasaki et al.[29]

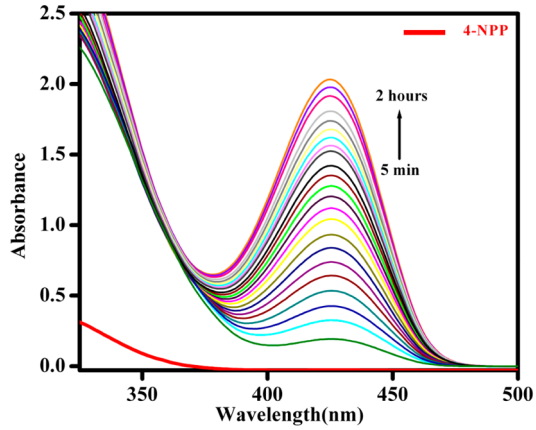

Figure 7. Wavelength scan for the hydrolysis of 4-NPP in the absence and presence of complex **1** (substrate:catalyst =20:1) in 97.5% DMF recorded at 25 °C at an interval of 5 min for 2 h. [4-NPP] = 1×10^{-3}(M), [Complex] = 0.05×10^{-3}(M). Arrow shows the change in absorbance with reaction time.

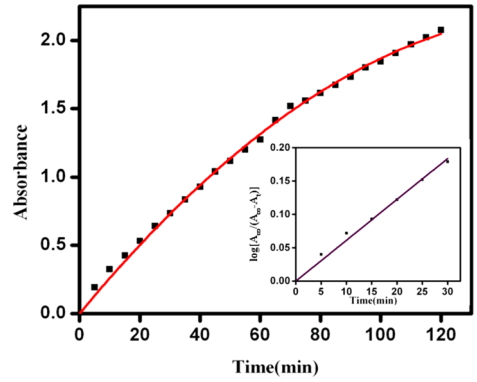

Figure 8. Absorption profile on addition of 4-NPP to complex-**1** due to the formation of *p*-nitrophenolate (λ_{max} = 427 nm) studied for 2 h (Least-squares fit, R^2 = 0.998). Inset shows the plot of log $[A_\infty/(A_\infty - A_t)]$ versus time for 30 min (R^2 = 0.99).

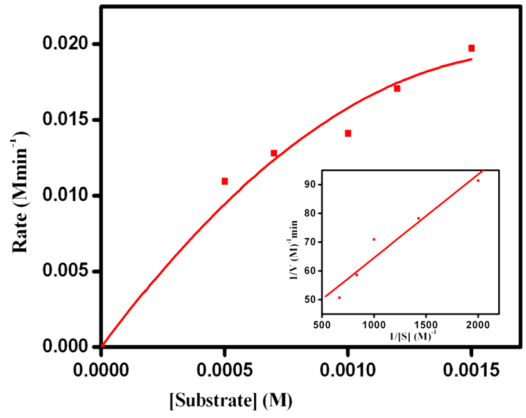

Figure 9. Plot of enzymatic kinetics for complex-**1** (V vs S, R^2 = 0.975). Inset shows the Lineweaver−Burk plot ($1/V$ vs $1/S$) having intercept = 35.62867 (error = 5.59117), slope = 0.02896 (error = 0.00437) and R^2 = 0.936.

Crystal Structure Determinations. *Dinuclear Complexes* ***1*****−****3.*** All dinuclear complexes are isostructural, and compounds **2**−**3** are also isomorphous, crystallizing in the same space group $P2_1/c$. The X-ray structural analysis revealed that in complexes

dx.doi.org/10.1021/ic4015493 | *Inorg. Chem.* 2014, 53, 85−96

Table 5. First-Order Rate Constants for Phosphatase Activity Obtained by Michaelis–Menten Treatment of Complex 1–6

complex	k_{cat} (sec^{-1})
1	9.35
2	8.80
3	8.33
4	4.68
5	3.29
6	2.88

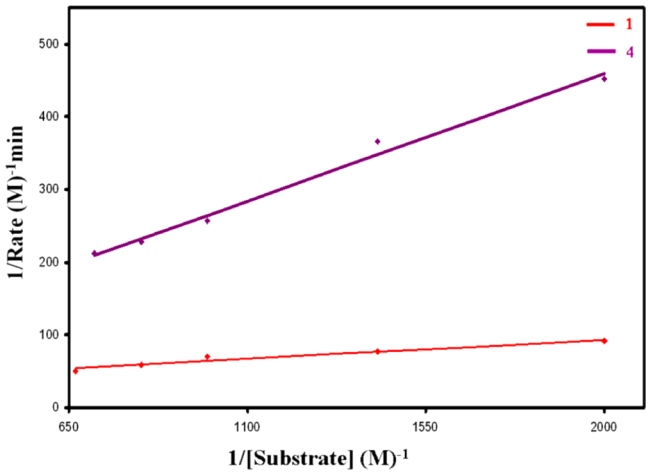

Figure 10. Overlay of the Lineweaver–Burk curve of a dinuclear (**1**) and a mononuclear (**4**) complex having the same halide substitution (Cl^-).

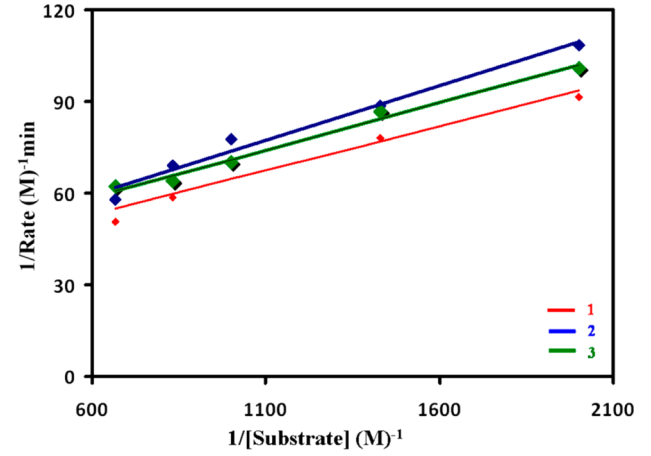

Figure 11. Overlay of the Lineweaver–Burk curve of dinuclear series (**1**, **2**, and **3**).

1–3 the metal ions are bridged by two phenolato units in a centrosymmetric fashion forming a four-membered Zn_2O_2 core. The ORTEP drawing of complex **1** is shown in Figure 2 (ORTEP of **2** and **3** is given in Supporting Information, Figure S18 and S19). A selection of coordination bond lengths and angles are reported in Table 2.

The Zn atoms complete their coordination sphere with the amino nitrogen, a halide, and an oxygen from one of the methoxyethyl arms, in a distorted trigonal bipyramidal geometry for which a trigonality τ index[44] of 0.60 is derived for **1–3**. Thus, the organic species acts as a chelating tridentate ligand toward each Zn ion, and in addition the phenoxo oxygen

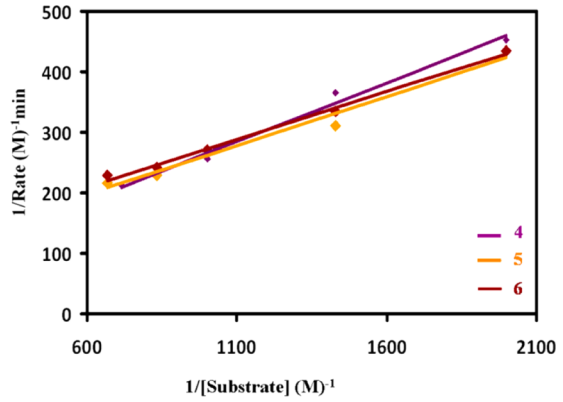

Figure 12. Overlay of the Lineweaver–Burk curve of mononuclear series (**4**, **5**, and **6**).

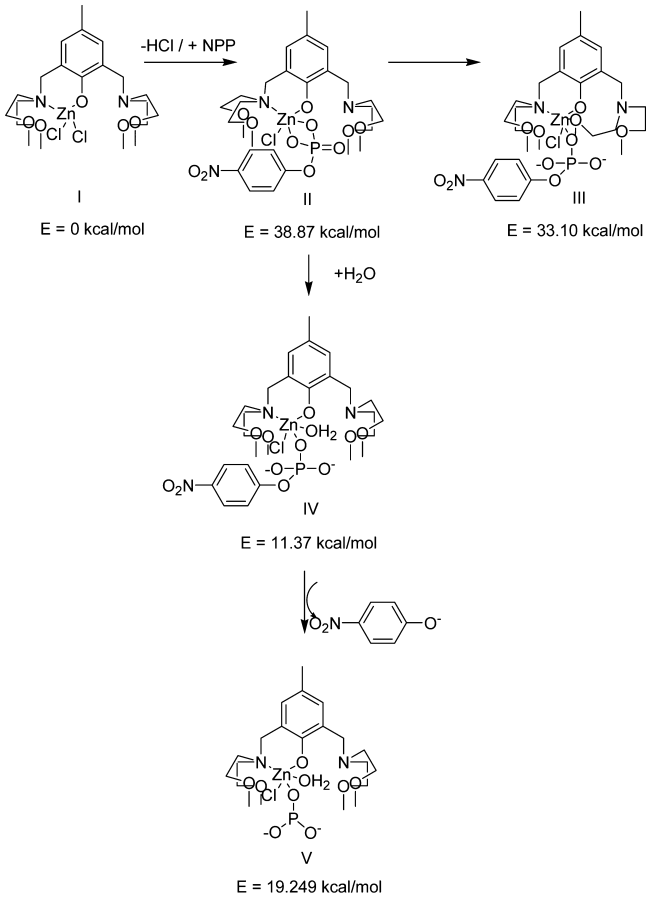

Figure 13. Schematically depicted plausible mechanism for the complex **4** as a representative of mononuclear (**4–6**) catalyzed hydrolytic pathway.

connects the other metal, so that one of the methoxyethyl arms remains uncoordinated evidencing a slight disorder as found in the crystal structure of **1** and **2** (see Experimental Section) or large thermal ellipsoids in **3** of these chain atoms. Because of the local symmetry, the halide ligands as well as the amine N atoms are located trans with respect to the Zn_2O_2 rhomboid mean plane.

In **1–3** the Z-N and Zn–O distances follow a regular trend showing decreasing values ongoing from the chloro to the iodo derivative (Table 2). However, it is worth noting that the Zn–O(2) bond distances (involving the coordinated methoxy

dx.doi.org/10.1021/ic4015493 | Inorg. Chem. 2014, 53, 85–96

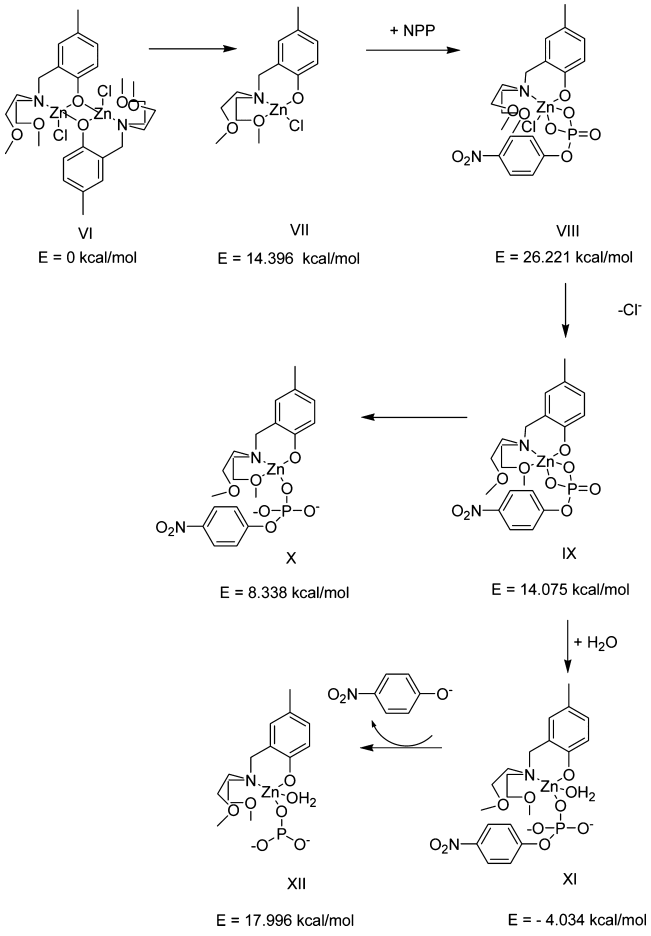

Figure 14. Schematically depicted plausible mechanism for complex **1** as a representative of the dinuclear (**1**−**3**) catalyzed hydrolytic pathway.

group) are significantly longer by 0.3 Å with respect to the other Zn−O distances of the bridging phenolato oxygens. On the other hand, the Zn-halide bond lengths augment along the series, following the expected trend of 2.2068(6), 2.3412(9), and 2.5085(13) Å in **1**−**3**, respectively. The decreasing values of coordination distances is also reproduced in the metal−metal distance: these values vary from 3.1081(4) and 3.1032(11) Å in **1** and **2**, respectively, and to 3.071(2) Å measured in **3**.

Mononuclear Complex ***4***. The mononuclear entity of complex **4** was verified by the X-ray structural analysis. The ORTEP view of **4** is shown in Figure 3. The metal presents in the complex a distorted tetrahedral coordination environment being chelated by the phenolato ligand and by two monocoordinated halides. The ethylmethoxy fragments of the organic ligands point far away from the metal center. The Zn−O and Zn−N bond lengths and their esd's are 1.926(3) Å and 2.0917(17) Å, respectively (Tables 2 and 3). It is worth to compare these distances with those found in the dinuclear species $[Zn_2(L^2)(MeCO_2)_2]^+$.[29] Here the phenolato oxygen bridge two hexa-coordinated zinc ions with Zn−O distances averaging to 1.999(4) Å, and also the Zn−N distances are significantly longer 2.147(4) Å likely to allow the methoxy oxygen atoms to be coordinated.

The two Zn−Cl distances, averaging at 2.23 Å, are just slightly longer than that found in the dinuclear species **1**. The chelating angle N(1)−Zn−O(1) of about 94° deviates significantly from the ideal tetrahedral value, while the other

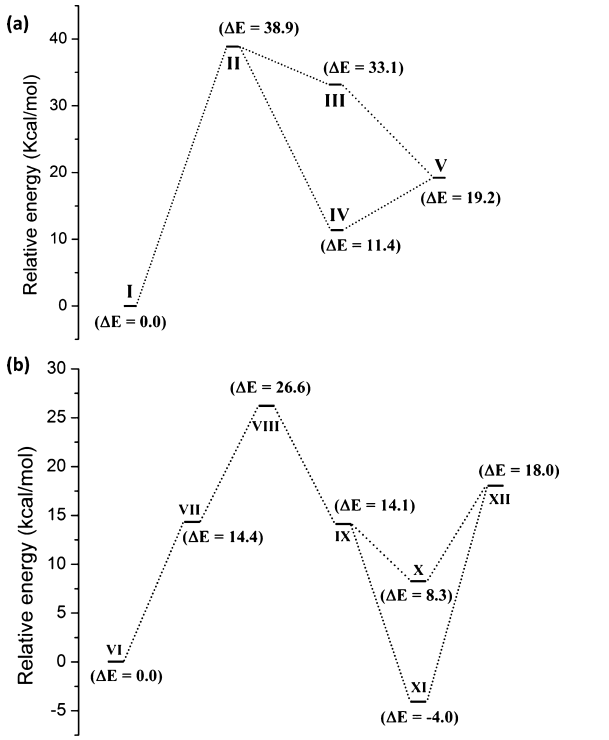

Figure 15. Energy profile diagrams: (a) mononuclear complex **4** and (b) dinuclear complex **1**.

angles fall in a range from 106.40(12) to 116.24(5)° in the three complexes. The metal ions reside almost in the phenolato plane (max deviation of 0.161(5) Å in **4**), and the coordinated amino N results displaced by about 0.75 Å from it. The structural determination confirms that the amino nitrogen on the other arm of the ligand is protonated and hampers, as suggested in the discussion, the coordination of a second metal ion. Although the geometry does not indicate a suitable alignment of the N−H···O fragment, the N(2)···O(1) distance is of about 2.67 Å in all cases favoring an intramolecular interaction (Table 4). The crystal packing does not manifest any peculiar feature.

NMR Spectral Properties. The proton NMR spectra of both ligands HL^1 and HL^2 in $CDCl_3$ show 5 signals in the aliphatic region consisting of 3 singlets and 2 triplets. At the aromatic region, for HL^1 one singlet peak at δ7.26 and two doublets at δ7.2 and δ7.43 are observed, whereas for HL^2 the two equivalent aromatic protons resonate at δ6.96 (Supporting Information, Figure S11−14). The proton spectra of the metal-complexes **1**−**6** were taken in DMF-d_7 which has a base peak at δ8.1 and δ3.7. The dinuclear ones (**1**−**3**) have similar type of spectra as HL^1 with slightly shifted values (4 singlets, 2 doublets, and 2 triplets) and mononuclear (**4**−**6**) are comparable to HL^2 (5 singlets and 2 triplets). The proton which binds to the uncoordinated tertiary nitrogen in **4**−**6** is probably abstracted by the basic solvent and does not appear in the deshielding zone (Supporting Information, Figures S15−S18). Comparing the spectra of ligand and complex we find that there is not much difference because not only that zinc is a diamagnetic center, the coordinated and uncoordinated methoxy groups have almost the same kind of magnetic environment. Thus from all the assignments it appears that the solution state structural formulations are in good agreement with their crystalline form.

dx.doi.org/10.1021/ic4015493 | *Inorg. Chem.* 2014, 53, 85−96

Table 6. First-Order Rate Constants for the Hydrolysis of Various Phosphate Esters by Previously Reported Zn^{II} Complexes[a]

complex	substrate	conditions	k_{cat} (s^{-1})	reference
$[Zn_2L]$	NPP	acetonitrile−water, pH 6.8, 25 °C	476−203	50
$[Zn_2(L2O)]$	HPNP	pH 6−6.5, 25 °C	4.10×10^{-3}	55
$[Zn^{II}_2(L^2)\text{-}(\mu\text{-}O_2CMe)_2(MeCN)_2][PF_6]$	HPNP	methanol−water (33%, v/v), 30 °C	3.44×10^{-4}	51
$[MPGN\text{-}Zn^{II}]$	BNPP	water−methanol (93:7), 40 °C	3.60×10^{-5}	56
$[Zn_2(LH_{-2})]^{2+}$	BNPP	water, 35 °C	2.26×10^{-6}	57
$[Zn_2(L_{2H})(AcO)(H_2O)](PF_6)] \cdot 0.2H_2O$	BNPP	methanol−water (1:5), pH 7.2, 50 °C	4.60×10^{-6}	52
$[Zn_2complex]$	HPNP	DMSO/buffered water (1:1), 50 °C	4.00×10^{-7}	58
$[Zn(bpy)Cl_2]$	BNPP	water, 25 °C	5.74×10^{-7}	59
$[Zn_2PBTPA]^+$	BNPP	30% DMSO, 55 °C	2.30×10^{-8}	60

[a]BNPP = Bis(4-nitrophenyl)phosphate. HPNP = 2-Hydroxypropyl(4-nitrophenyl)-phosphate.

Electronic Properties. The absorption spectra of the ligands in DMF (Figure 4) show two higher energy bands of high intensity in the region 250−285 nm which is attributed to the intraligand charge transfer of the open and closed forms of hydrogen-bonded species and also a lower energy band (330−430 nm) of lower intensity owing to the zwitterionic form of the ligand. The complexes display one/two intraligand charge transfer band(s) in 235−265 nm (high energy) and a ligand to metal charge transfer band at ∼285 nm (low energy) which is probably due to $PhO^- \rightarrow Zn^{II}$ or admixture of the former and $X^- \rightarrow Zn^{II}$ (Figure 5).[45−47] The spectra remains almost same when measured in 97.5% DMF and therefore is not given separately.

The solid-state absorption spectra of the complexes exhibit peaks in the same region (Supporting Information, Figure S19 and S20).

Solution State Structures. ESI-MS spectra of the complexes indicate a base peak corresponding to the presence of a mononuclear unit for the dinuclear complexes (**1**−**3**) and a monodehalogenated species for the mononuclear ones (**4**−**6**) as depicted in Supporting Information, Figure S21 and S22 for complex **1** and **4**, respectively. Molar conductance studies in 97.5% DMF at pH 6 prove all the complexes are nonelectrolyte (values are provided in Supporting Information, Table S1).[46,48,49] The UV−vis spectra of the complexes in the solid and solution phase remains more or less unaltered suggesting no major change in the basic chromophore of the molecules. Nevertheless the spectral nature of a dinuclear and a mononuclear complex in DMF is very similar emphasizing a close resemblance in their structures in solution. Thus according to our observations, in solution, a dinuclear complex probably dissociates into two equivalent mononuclear moieties whereas a mononuclear complex loses an HX molecule (X = $Cl^-/Br^-/I^-$, proton from the uncoordinated nitrogen and halide ion from the zinc) having structures as shown in Figure 6. Thus in either case the absorption spectra is not much perturbed.

Hydrolysis of Phosphomonoester in DMF-Buffered H_2O. To study the phosphatase activity of the zinc complexes, disodium salt of (4-nitrophenyl)phosphate hexahydrate was chosen as the substrate. Their hydrolytic tendency was detected spectrophotometrically by monitoring the time evolution of *p*-nitrophenolate (λ_{max} = 427 nm) through wavelength scan from 200 to 800 nm in aqueous DMF (DMF:water = 97.5:2.5) where substrate was in 20 equivalents of the catalyst, till roughly 2% reaction conversion. The change in spectral behavior of complex **1** is shown in Figure 7 as a representative of dinuclear complexes and of **4** (Supporting Information, Figure S23) for mononuclear ones.

Kinetic Studies. The kinetic study of complexes **1**−**6** was done by the initial slope method following the rate of increase in absorption of the band at ∼427 nm corresponding to a rise in 4-nitrophenolate concentration. The initial first-order rate constants, V (min^{-1}), for the cleavage of NPP were obtained directly from the plot of $\log[A_\infty/(A_{\infty\alpha} - A_t)]$ values versus time (through origin) which were linear with $R^2 \geq 0.99$. A typical plot of that kind is represented in the inset of Figure 8 for complex **1** (and Supporting Information, Figure S24 for complex **4**) along with the change in its absorbance profile at 427 nm for the concentration used in the wavelength scan (Figure 7). To determine the dependence of rate constants on substrate concentration, **1**−**6** were treated with five different concentrations of substrate. As can be observed for each complex, initially the cleavage rate increases linearly with the increase of 4-NPP concentration but deviates gradually from linearity and finally tends toward a saturation curve (Figure 9). In other words, it is a first order kinetics at lower concentration which gradually differs from unity at higher concentration. The kinetic parameters (V_{max}, k_M, k_{cat}) for the catalyzed reactions were determined from the linear plots of $1/V$ versus $1/[NPP]$ values (Lineweaver−Burk plot) as per the Michaelis−Menten approach of enzymatic kinetics. Similar plots for **2**−**6** are given in Supporting Information, Figures S25−S29. The results of calculation remained the same when the experiment was done by varying the [complex] under investigation at constant [NPP]. All the kinetic parameters are given in Supporting Information, Table S2, and only the k_{cat} values are summarized in Table 5.

To correct for the spontaneous cleavage of 4-NPP, each reaction was measured against a reference cell that was identical to the sample cell in composition except for the absence of Zn complex. The spontaneous hydrolysis of 4-NPP had a much lower reaction rate when compared to the metal catalyzed reaction and hence the rate of spontaneous hydrolysis of 4-NPP was too low to be taken into account in the kinetic measurements. Therefore, the general rate of spontaneous hydrolysis was not separately determined.[49]To confirm that the synthesized ligands and the zinchalide-salts used do not participate in the catalytic reaction, rigorous control experiments have been performed to intake their role if any (Supporting Information, Figures S30−S32). The results indicated no appreciable change.

The kinetic data shows very clearly that the first-order rate constants (k_{cat}) follow the order of **1** > **2** > **3** > **4** > **5** > **6**. This indicates that the dinuclear compounds (**1**−**3**) are better catalysts for phosphate ester hydrolysis than mononuclear ones (**4**−**6**) (Figure 10) as supported by Konig et al.,[21] Kandaswamy et al.,[50] Mukherjee et al.[51] and more interestingly, in both cases,

dx.doi.org/10.1021/ic4015493 | Inorg. Chem. 2014, 53, 85−96

halide dependence follows the order chloride > bromide > iodide (Figure 11 and 12).

The commonly accepted mechanism of the metal ion catalyzed hydrolysis of phosphate esters involves the following key steps: deprotonation of a metal-bound species to form the effective nucleophile, binding of the substrate to the metal center(s), intramolecular nucleophilic attack on the electrophilic phosphorus atom with the release of the leaving group, and possibly regeneration of the catalyst.[51] Thus to begin with, first and foremost, the zinc(II) core recognizes and binds the phosphate bond through coordinate linkage and electrostatic interaction. Then it activates and nucleophilically attacks the central phosphorus atom by a metal-bound external water/hydroxide ion or the proximally bound methoxy group generating a trigonal bipyramid phosphorus intermediate from where the P−O ester bond is finally cleaved. Now the latter possibility of the nucleophilic attack is geometrically and electronically much less favorable. Therefore we have neatly established a classical Lewis acid activation mechanism where Zn(II)-coordinated H_2O/OH^- is the sole nucleophile, and an increase in Lewis-acidity of the metal ion enhances the acidity of the M^{II}-coordinated water which in turn magnifies the propensity of the metal ion to catalyze the hydrolysis of an activated phosphate ester 4-NPP.

To rationalize the mechanistic pathway involved in phosphatase activity we have performed detailed DFT calculations considering complex **1** and complex **4** as representatives of di- and mononuclear series respectively.

Along with the knowledge gathered from the literature survey[24,46−54] and the results obtained from DFT calculations we have put forward the most probable mechanistic pathway involved in mono- and dinuclear complex catalyzed reactions as depicted in Figures 13 and 14, respectively. In case of a mononuclear complex, the reaction is initiated by an association of the substrate and metallocatalyst (intermediate **II**) with a loss of halide ion. For the dinuclear complexes, the reaction is initiated by the dissociation of the dinuclear (**I**) to mononuclear species (**II**), association of the substrate molecule in a *cis*-bidentate fashion (**III**) and loss of the halide ion (**IV**). This is followed by an intramolecular nucleophilic attack by a pendant methoxy group on the zinc center (**III** for monomer and **X** for dimer) or the direct addition of a water molecule on the zinc ion (**IV** for monomer and **XI** for dimer). Formations of **IV** and **XI** (in case of mono- and dinuclear complexes, respectively) are energetically more favorable than their respective counterparts **III** and **X**, formed by intramolecular nucleophilic attack by a pendant methoxy group. In the final step P−O bonds present in **IV** and **XI** undergo hydrolytic cleavage due to nucleophilic attack by internal water molecules leading to elimination of *p*-nitrophenolate and simultaneous aquation generating the intermediates **V** and **XII**. The subsequent dissociation of the reactive species from **V** and **XII** regenerate the active catalyst to continue the catalytic cycle. The concentration of active species involved in case of the dinuclear complex is double that of the mononuclear complex since one molecule of dinuclear species generates two mononuclear species and that particular consequence is supposed to be responsible for nearly double reactivity (in terms of k_{cat}) of dinuclear complexes over their respective mononuclear counterparts. The role of halide is attributed to their electron-withdrawing inductive effect which improves the electrophilicity of the metal center thus enhancing its hydrolytic reactivity. So the halide effect is actually their electronegativity order.

To get a better visualization of the energetically viable mechanistic pathway proposed by us we have represented the relative energies of the intermediates as the conventional energy-profile diagrams, which are depicted in Figure 15a and 15b (for mononuclear complex **4** and dinuclear complex **1**, respectively).

Understandably, the k_{cat} value of a dinuclear:mononuclear is approximately 2 for all the three halide groups. For **1**:**4** it is exactly equal to 2, for **2**:**5** it is 2.7, and for **3**:**6** it is 2.9. Moreover the ratio of k_{cat} for **1**:**2**:**3** = 1.12:1.06:1 whereas for **4**:**5**:**6** = 1.62:1.14:1. This is quite anticipated as reactivity has an inverse relationship with selectivity, and as the halides move toward electropositive character, the halide effect becomes more and more prominent and hence the rate of decrease in k_{cat} value for mononuclear complexes increases.

It is now essential to compare the catalytic efficiency of our Zn-complexes as hydrolytic catalyst with the previously reported analogous Zn complexes in terms of k_{cat} values. Table 6 represents the hydrolytic rate constants of all recently reported Zn complexes along with their relevant references. Now on comparing Table 5 and Table 6 it can be safely commented that our Zn complexes belong to the group of complexes showing the highest catalytic efficiency reported till date.

CONCLUSIONS

An unprecedented Mannich reaction has been identified while synthesizing the ligand where one of the two products is a conventional intermediate in this age-old synthetic reaction. It can henceforth be applicable to generate a mononucleating and dinucleating ligand simultaneously on a similar organic backbone. The metalation strategy also depicted an interesting phenomenon where the nuclearity feature was prominently reversed. The three dinuclear and three mononuclear Zn^{II} complexes so formed have been found to be efficient monophosphatase catalysts. The kinetic parameters are quite higher than most of the values reported till date under our experimental conditions. The role of the coligand which is a halide has been investigated, established, and reasoned. The influence follows the order: $Cl^- > Br^- > I^-$, irrespective of the nuclearity of the catalysts in solid state. A classical hydrolytic pathway for the phosphatase activity has been proposed on the basis of our experimental observations, and DFT analyses have been performed to rationalize our proposition. Influences of other metal ions in the same ligand environment on phosphatase-like activity are also under process.

ASSOCIATED CONTENT

Supporting Information

X-ray crystallographic data in CIF format of complexes **1**−**4**, ORTEP diagrams, kinetic plots, and FTIR, NMR, UV−vis, ESI-MS spectroscopic data and DFT optimized energies of different intermediates. This material is available free of charge via the Internet at http://pubs.acs.org.

AUTHOR INFORMATION

Corresponding Authors

*E-mail: zangrando@units.it (E.Z.).
*E-mail: dasdebasis2001@yahoo.com (D.D.).

Notes

The authors declare no competing financial interest.

■ ACKNOWLEDGMENTS

This research is funded by the Council of Industrial and Scientific Research, New Delhi [CSIR project no. 01(2464)/11/EMR-II dated 16-05-2011 to D.D.]. R.S. is thankful to CSIR-SRF fellowship for financial support and Pujarini Banerjee of IACS for ESI-MS measurements. We are also thankful to Dr. D. K. Maiti for assistance in NMR experiments.

■ REFERENCES

(1) Vallee, B. L.; Galdes, A. *Adv. Enzymol. Relat. Areas Mol. Biol.* **1984**, *56*, 283−430.
(2) Vallee, B. L.; Auld, D. S. In *Matrix Metalloproteinases and Inhibitors*; Birkedal-Hansen, H., Werb, Z., Welgus, H., Van Wart, H., Eds.; Gustav Fischer: Stuttgart, Germany, 1992; pp 5−19.
(3) Vallee, B. L.; Auld, D. S. *Acc. Chem. Res.* **1993**, *26*, 543−551.
(4) Hambidge, M.; Krebs, N. *J. Pediatr.* **1999**, *135*, 661−664.
(5) (a) Eby, G. A. *J. Antimicrob. Chemother.* **1997**, *40*, 483−493. (b) Gadomski, A. *J. Am. Med. Assoc.* **1998**, *279*, 1999−2000. (c) Macknin, M. L.; Piedmonte, M.; Calendine, C.; Janosky, J.; Wald, E. *J. Am. Med. Assoc.* **1998**, *279*, 1962−1967. (d) Macknin, M. L. *Cleveland Clin. J. Med.* **1999**, *66*, 27−32. (e) Barceloux, D. G. *J. Toxicol. Clin. Toxicol.* **1999**, *37*, 279−292. (f) Petrus, E. J.; Lawson, K. A.; Bucci, L. R.; Blum, K. *Curr. Ther. Res.* **1998**, *59*, 595−607. (g) Bakar, N. K. A.; Taylor, D. M.; Williams, D. R. *Chem. Speciation Bioavailability* **1999**, *11*, 95−101. (h) Williams, D. R. *Coord. Chem. Rev.* **1999**, *186*, 177−188.
(6) Parkin, G. *Chem. Rev.* **2004**, *104*, 699−767.
(7) (a) Vallee, B. L.; Auld, D. S. *Proc. Natl. Acad. Sci. U.S.A.* **1990**, *87*, 220−224. (b) Vallee, B. L.; Auld, D. S. *Biochemistry* **1990**, *29*, 5647−5659. (c) Vallee, B. L.; Auld, D. S. *Proc. Natl. Acad. Sci. U.S.A.* **1993**, *90*, 2715−2718. (d) Auld, D. S. *Struct. Bonding (Berlin)* **1997**, *89*, 29−50. (e) Vallee, B. L.; Auld, D. S. *Biochemistry* **1993**, *32*, 6493−6500. (f) Vallee, B. L.; Falchuk, K. H. *Physiol. Rev.* **1993**, *73*, 79−118. (g) Turner, A. J. *Biochem. Soc. Trans.* **2003**, *31*, 723−727.
(8) (a) Lipscomb, W. N. *Annu. Rev. Biochem.* **1983**, *52*, 17−34. (b) Lipscomb, W. N.; Sträter, N. *Chem. Rev.* **1996**, *96*, 2375−2433. (c) Christianson, D. W.; Lipscomb, W. N. *Mol. Struct. Energ.* **1988**, *9*, 1−25.
(9) (a) Coleman, J. E. *Annu. Rev. Biochem.* **1992**, *61*, 897−946. (b) Coleman, J. E. *Curr. Opin. Chem. Biol.* **1998**, *2*, 222−234.
(10) Rahuel-Clermont, S.; Dunn, M. F. The biological chemistry of zinc. In *Copper and Zinc in Inflammatory and Degenerative Diseases*; Rainsford, K.D., Milanino, R., Sorenson, J. R. J., Velo, G. P., Eds.; Kluwer Academic Publications: Boston, MA, 1998; pp 47−59.
(11) Mills, C. F. *Zinc in Human Biology*; Springer-Verlag: New York, 1989.
(12) Wilcox, D. E. *Chem. Rev.* **1996**, *96*, 2435−2458.
(13) Sträter, N.; Lipscomb, W. N.; Klabunde, T.; Krebs, B. *Angew. Chem., Int. Ed. Engl.* **1996**, *35*, 2024−2055.
(14) Horton, N. C.; Perona, J. J. *Nat. Struct. Biol.* **2001**, *8*, 290−293.
(15) Cowan, J. A. *Chem. Rev.* **1998**, *98*, 1067−1087.
(16) (a) Kimura, E.; Koike, T. *Adv. Inorg. Chem.* **1997**, *44*, 229−261. (b) Coleman, J. E. *Curr. Opin. Chem. Biol.* **1998**, *2*, 222−234.
(17) Bauer-Siebenlist, B.; Meyer, F.; Farkas, E.; Vidovic, D.; Dechert, S. *Chem.—Eur. J.* **2005**, *11*, 4349−4360.
(18) (a) Kimura, E. *Acc. Chem. Res.* **2001**, *34*, 171−179. (b) Kimura, E.; Kikuta, E. *J. Biol. Inorg. Chem.* **2000**, *5*, 139−155. (c) Vahrenkamp, H. *Acc. Chem. Res.* **1999**, *32*, 589−596. (d) Vahrenkamp, H. *Bioinorganic Chemistry: Transition Metals in Biology and their Coordination Chemistry*; Wiley-VCH: Weinheim, Germany, 1997; pp 540−551. (e) Kimura, E.; Koike, T.; Shionoya, M. *Struct. Bonding (Berlin, Ger.)* **1997**, *89*, 1−28. (f) Kimura, E.; Koike, T. *Adv. Inorg. Chem.* **1997**, *44*, 229−261. (g) Brown, R. S.; Huguet, J.; Curtis, N. J. *Met. Ions Biol. Syst.* **1983**, *15*, 55−99. (h) Brown, R. S. *NATO Adv. Study Inst. Ser., Ser. C* **1990**, *314*, 145−180. (i) Brown, R. S. *NATO Adv. Study Inst. Ser., Ser. C* **1987**, *206*, 169−197. (j) Banci, L.; Bertini, I.; Luchinat, C.; Moratal, J. M. *NATO Adv. Study Inst. Ser., Ser. C* **1990**, *314*, 181−197. (k) Bertini, I.; Luchinat, C.; Monnanni, R. *NATO Adv. Study Inst. Ser., Ser. C* **1987**, *206*, 139−167. (l) Kimura, E. *Pure Appl. Chem.* **1993**, *65*, 355−359. (m) Zongwan, M.; Liangnian, J. *Prog. Chem.* **2002**, *14*, 311−317. (n) Parkin, G. *Met. Ions Biol. Syst.* **2001**, *38*, 411−460. (o) Parkin, G. *Chem. Commun.* **2000**, 1971−1985. (p) Elsevier, C. J.; Reedijk, J.; Walton, P. H.; Ward, M. D. *Dalton Trans.* **2003**, 1869−1880.
(19) Kimura, E. *Prog. Inorg. Chem.* **1994**, *41*, 443−491.
(20) Jedrjezas, M. J.; Setlow, P. *Chem. Rev.* **2001**, *101*, 607−618.
(21) Subat, M.; Woinaroschy, K.; Gerstl, C.; Sarkar, B.; Kaim, W.; Konig, B. *Inorg. Chem.* **2008**, *47*, 4661−4668.
(22) (a) Zalatan, J. G.; Herschlag, D. *J. Am. Chem. Soc.* **2006**, *128*, 1293−1303. (b) Weston, J. *Chem. Rev.* **2005**, *105*, 2151−2174. (c) Mancin, F.; Tecilla, P. *New J. Chem.* **2007**, *31*, 800−817. (d) Aubert, S. D.; Li, Y.; Raushel, F. M. *Biochemistry* **2004**, *43b*, 5707−5715. (e) Morrow, J. R. *Comments Inorg. Chem.* **2008**, *29*, 169−188.
(23) Raycroft, M. A. R.; Tony Liu, C.; Brown, R. S. *Inorg. Chem.* **2012**, *51*, 3846−3854.
(24) (a) Hegg, E. L.; Burstyn, J. N. *Coord. Chem. Rev.* **1998**, *173*, 133−165. (b) Suh, J. *Acc. Chem. Res.* **1992**, *25*, 273−279.
(25) Göbel, M. W. *Angew. Chem., Int. Ed. Engl.* **1994**, *33*, 1141−1143.
(26) (a) Kovbasyuk, L.; Krämer, R. *Chem. Rev.* **2004**, *104*, 3161−3187. (b) Feng, G.; Mareque-Rivas, J. C.; de Rosales, R. T. M.; Williams, N. H. *J. Am. Chem. Soc.* **2005**, *127*, 13470−13471. (c) O'Donoghue, A. M.; Pyun, S. Y.; Yang, M.-Y.; Morrow, J. R.; Richard, J. P. *J. Am. Chem. Soc.* **2006**, *128*, 1615−1621.
(27) Kim, E. E.; Wyckoff, H. W. *J. Mol. Biol.* **1991**, *218*, 449−464.
(28) (a) For reviews, see: Chin, J. *Acc. Chem. Res.* **1991**, *24*, 145−152. (b) Liu, C.; Wang, M.; Zhang, T.; Sun, H. *Coord. Chem. Rev.* **2004**, *248*, 147−168. (c) Kruppa, M.; König, B. *Chem. Rev.* **2006**, *106*, 3520−3560.
(29) Sakiyama, H.; Mochizuki, R.; Sugawara, A.; Sakamoto, M.; Nishida, Y.; Yamasaki, M. *J. Chem. Soc., Dalton Trans.* **1999**, 997−1000.
(30) Sakiyama, H.; Sugawara, A.; Sakamoto, M.; Unoura, K.; Inoue, K.; Yamasaki, M. *Inorg. Chim. Acta* **2000**, *310*, 163.
(31) Sakiyama, H.; Ito, R.; Kumagai, H.; Inoue, K.; Sakamoto, M.; Nishida, Y.; Yamasaki, M. *Eur. J. Inorg. Chem.* **2001**, *8*, 2027.
(32) Sakiyama, H.; Suzuki, T.; Ono, K.; Ito, R.; Watanabe, Y.; Yamasaki, M.; Mikuriya, M. *Inorg. Chim. Acta* **2005**, *358*, 1897.
(33) Sakiyama, H.; Yamasaki, M.; Suzuki, T.; Watanabe, Y.; Ito, R.; Ohnishi, A.; Nishida, Y. *Inorg. Chem. Commun.* **2006**, *9*, 18.
(34) Shibayama, J.; Sakiyama, H.; Yamasaki, M.; Nishida, Y. *Anal. Sci.: X-Ray Struct. Anal. Online* **2008**, *24*, 177.
(35) *SMART, SAINT. Software Reference Manual*; Bruker AXS Inc.: Madison, WI, 2000.
(36) Sheldrick, G. M. *SHELXL-97, Programs for Crystal Structure Analysis*, Release 97-2; University of Göttingen: Göttingen, Germany, 1998.
(37) Farrugia, L. J. *J. Appl. Crystallogr.* **1999**, *32*, 837−838.
(38) Subat, M.; Woinaroschy, K.; Anthofer, S.; Malterer, B.; Konig, B. *Inorg. Chem.* **2007**, *46*, 4336.
(39) (a) Becke, A. D. *J. Chem. Phys.* **1993**, *98*, 5648−5652. (b) Lee, C.; Yang, W.; Parr, R. G. *Phys. Rev. B* **1988**, *37*, 785−789. (c) Stevens, P. J.; Devlin, J. F.; Chabalowski, C. F.; Frisch, M. J. *J. Phys. Chem.* **1994**, *98*, 11623−11627.
(40) Frisch, M. J.; Trucks, G. W.; Schlegel, H. B.; Scuseria, G. E.; Robb, M. A.; Cheeseman, J. R.; Montgomery, J. A.; Vreven, Jr.T.; Kudin, K. N.; Burant, J. C.; Millam, J. M.; Iyengar, S. S.; Tomasi, J.; Barone, V.; Mennucci, B.; Cossi, M.; Scalmani, G.; Rega, N.; Petersson, G. A.; Nakatsuji, H.; Hada, M.; Ehara, M.; Toyota, K.; Fukuda, R.; Hasegawa, J.; Ishida, M.; Nakajima, T.; Honda, Y.; Kitao, O.; Nakai, H.; Klene, M.; Li, X.; Knox, J. E.; Hratchian, H. P.; Cross, J. B.; Bakken, V.; Adamo, C.; Jaramillo, J.; Gomperts, R.; Stratmann, R. E.; Yazyev, O.; Austin, A. J.; Cammi, R.; Pomelli, C.; Ochterski, J. W.; Ayala, P. Y.; Morokuma, K.; Voth, G. A.; Salvador, P.; Dannenberg, J. J.; Zakrzewski, V. G.; Dapprich, S.; Daniels, A. D.; Strain, M. C.; Farkas, O.; Malick, D. K.; Rabuck, A. D.; Raghavachari, K.; Foresman, J. B.; Ortiz, J. V.; Cui, Q.; Baboul, A. G.; Clifford, S.; Cioslowski, J.; Stefanov, B. B.; Liu, G.; Liashenko, A.; Piskorz, P.; Komaromi, I.;

Martin, R. L.; Fox, D. J.; Keith, T.; Al-Laham, M. A.; Peng, C. Y.; Nanayakkara, A.; Challacombe, M.; Gill, P. M. W.; Johnson, B.; Chen, W.; Wong, M. W.; Gonzalez, C.; Pople, J. A. *Gaussian 03*, Revision D.01; Gaussian, Inc.: Wallingford, CT, 2004.
(41) Hay, P. J.; Wadt, W. R. *J. Chem. Phys.* **1985**, *82*, 270.
(42) (a) Liras, S.; Davoren, J. E.; Bordner, J. *Org. Lett.* **2001**, *3*, 703−706. (b) Ito, M.; Clark, C. W.; Mortimore, M.; Goh, J. B.; Martin, S. F. *J. Am. Chem. Soc.* **2001**, *123*, 8003−8010. (c) Deng, W.; Overman, L. E. *J. Am. Chem. Soc.* **1994**, *116*, 11241−11250.
(43) (a) Arend, M.; Westermann, B.; Risch, N. *Angew. Chem., Int. Ed.* **1998**, *37*, 1044−1070. (b) Overmann, L. E.; Ricca, D. J. *Comprehensive Organic Synthesis*; Trost, B. M., Fleming, I., Eds.; Pergamon Press: Oxford, U.K., 1991; Vol. *2*, pp 1007−1010.
(44) Addison, A. W.; Rao, T. N.; Reedijk, J.; Rijn, J. V.; Verschoor, G. C. *J. Chem. Soc., Dalton Trans.* **1984**, 1349.
(45) Annigeri, S. M.; Sathisha, M. P.; Revankar, V. K. *Transition Met. Chem.* **2007**, *32*, 81−87.
(46) Annigeri, S. M.; Naik, A. D.; Gangadharmath, U. B.; Revankar, V. K.; Mahale, V. B. *Transition Met. Chem.* **2002**, *27*, 316−320.
(47) Naik, A. D.; Revankar, V. K. *Proc. Indian Acad. Sci. (Chem. Sci.)* **2001**, *113*, 285−290.
(48) Brooker, S.; Davidson, T. C. *Chem.Commun.* **1997**, 2007−2008.
(49) Abe, K.; Izumi, J.; Ohba, M.; Yokoyama, T.; Okawa, H. *Bull. Chem. Soc. Jpn.* **2001**, *74*, 85−95.
(50) Anbu, S.; Kamalraj, S.; Varghese, B.; Muthumary, J.; Kandaswamy, M. *Inorg. Chem.* **2012**, *51*, 5580−5592.
(51) Arora, H.; Barman, S. K.; Lloret, F.; Mukherjee, R. N. *Inorg. Chem.* **2012**, *51*, 5539−5553.
(52) Chen, J.; Wang, X.; Zhu, Y.; Lin, J.; Yang, X.; Li, Y.; Lu, Y.; Guo, Z. *Inorg. Chem.* **2005**, *44*, 3422−3430.
(53) Bazzicalupi, C.; Bencini, A.; Berni, E.; Bianchi, A.; Fedi, V.; Fusi, V.; Giorgi, C.; Paoletti, P.; Valtancoli, B. *Inorg. Chem.* **1999**, *38*, 4115−4122.
(54) Goldberg, D. P.; diTargiani, R. C.; Namuswe, F.; Minnihan, E. C.; Chang, S.; Zakharov, L. N.; Rheingold, A. L. *Inorg. Chem.* **2005**, *44*, 7559−7569.
(55) Iranzo, O.; Kovalevsky, A. Y.; Morrow, J. R.; Richard, J. P. *J. Am. Chem. Soc.* **2003**, *125*, 1988−1993.
(56) Bonomi, R.; Selvestrel, F.; Lombardo, V.; Sissi, C.; Polizzi, S.; Mancin, F.; Tonellato, U.; Scrimin, P. *J. Am. Chem. Soc.* **2008**, *130*, 15744−15745.
(57) Vichard, C.; Kaden, T. A. *Inorg. Chim. Acta* **2002**, *337*, 173−180.
(58) Penkova, L. V.; Macia-g, A.; Rybak-Akimova, E. V.; Haukka, M.; Pavlenko, V. A.; Iskenderov, T. S.; Kozzowski, H.; Meyer, F.; Fritsky, I. O. *Inorg. Chem.* **2009**, *48*, 6960−6971.
(59) He, J.; Sun, J.; Maoa, Z.−W.; Ji, L.−N.; Sun, H. J. *Inorg. Biochem.* **2009**, *103*, 851−858.
(60) Zhu, L.; Santos, O.; Koo, C. W.; Rybstein, M.; Pape, L.; Canary, J. W. *Inorg. Chem.* **2003**, *42*, 7912−7920.

dx.doi.org/10.1021/ic4015493 | *Inorg. Chem.* 2014, 53, 85−96